Jurnal
Teknologi

Full Paper

DEVELOPMENT AND VERIFICATION OF A 9-DOF ARMORED VEHICLE MODEL IN THE LATERAL AND LONGITUDINAL DIRECTIONS

Vimal Rau Aparow[a*], Khisbullah Hudha[a], Megat Mohamad Hamdan Megat Ahmad[a], Hishamuddin Jamaluddin[b]

[a]Department of Mechanical Engineering, Faculty of Engineering, National Defense University of Malaysia, Kem Sungai Besi, Kuala Lumpur, Malaysia
[b]Department of Applied Mechanics and Design, Faculty of Mechanical Engineering, Universiti Teknologi Malaysia, 81310 UTM Johor Bahru, Johor, Malaysia

Article history
Received
19 Sepember 2015
Received in revised form
28 October 2015
Accepted
15 May 2016

*Corresponding author
vimalrau87vb@gmail.com

Abstract

This manuscript presents the development of an armored vehicle model in lateral and longitudinal directions. A Nine Degree of Freedom (9-DOF) armored vehicle model was derived mathematically and integrated with an analytical tire dynamics known as Pacejka Magic Tire model. The armored vehicle model is developed using three main inputs of a vehicle system which are Pitman arm steering system, Powertrain system and also hydraulic assisted brake system. Several testings in lateral and longitudinal direction are performed such as double lane change, slalom, step steer and sudden acceleration and sudden braking to verify the vehicle model. The armored vehicle model is verified using validated software, CarSim, using HMMWV vehicle model as a benchmark. The verification responses show that the developed armored vehicle model can be used for both lateral and longitudinal direction analysis

Keywords: 9-DOF, armored vehicle, lateral, longitudinal, HMMWV vehicle

Abstrak

Manuskrip ini membentangkan mengenai permodelan kenderaan kereta kebal pada arah ke sisi dan mendatar. Sembilan darjah kebebasan (9-DOF) model kenderaan kereta kebal telah diperoleh secara matematik dan bersepadu dengan dinamik tayar analisis dikenali sebagai model Pacejka Magic tayar. Model kenderaan kereta kebal itu juga dibangunkan dengan menggunakan tiga input utama system untuk kenderaan iaitu *Pitman Arm* sistem stereng, sistem enjin dan juga sistem brek dengan menggunakan system hydralik. Beberapa ujian ke arah sisi dan memdatar telah dianalisasi dalam manuscript ini seperti perubahan dua lorong, *Slalom* , langkah kemudi dan pecutan dan brek secara tiba-tiba untuk mengesahkan kesahihkan model kenderaan tersebut. Model kenderaan ini dianalisasikan dengan menggunakan system perisian yang disahkan, iaitu *CarSim* , dengan menggunakan kenderaan kereta kebal HMMWV sebagai rujukan utama. Hasil ujian-ujian ini menunjukkan bahawa model kenderaan kereta kebal yang dibangunkan boleh digunakan untuk menganalisasi ciri-ciri sebuah kenderan kereta kebal pada kedua-dua arah iaitu sisi dan mendatar.

Kata kunci: Sembilan darjah kebebasan, kereta kebal, sisi, memdatar, kereta HMMWV

1.0 INTRODUCTION

Since past few decades, vehicle plays an important role for every human in their daily life usage. Owning personal vehicles not only will reduce time but also save human energy to travel from one location to another. However, this transportation has significantly increased the risk of each human's life due to road accidents. The major cause of the vehicle accidents is the non-stability conditions of a vehicle where the drivers lost control while driving either by steering, throttle or braking input [1]. Rollover and skidding are known as a major effect occurs once the driver unable to control the vehicle. Therefore, handling and stability of each vehicle has become one of the main priorities for the automotive developers during analysis procedure.

The handling and stability performances are one of the important milestones in developing a vehicle. In order to reduce time and also the costing issue, the automotive developers initiate their research works by developing a vehicle model via computer-based simulation technique. Most of the automotive researchers developed the vehicle model using mathematical derivation by describing them in terms of degree of freedom (DOF). The advantage of using this computer-based simulation technique is to study and analyze the dynamic behavior of a vehicle system by simulating into a mathematical model. The simulation model can be evaluated using various types of operating conditions and also able to make appropriate adjustment to the vehicle model for future improvement [2]. The simulation technique also has great significance in reducing the cost for test bed and testing instruments as for initial stage of analysis since it does not require in simulation techniques [3].

In recent years, most of the automotive researchers extensively involved in the development of vehicle model to analysis the dynamic behavior of an actual vehicle. They have developed the vehicle model as a simplified quarter and half vehicle model or full vehicle model. In term of quarter vehicle model in vertical direction, previous researchers have done evaluation on the suspension system. Yoshimura *et al.* [4] successfully developed an active suspension system of a quarter vehicle model using sliding mode control. Meanwhile, Litak *et al.* [5] and Turkay and Akcay [6] studied on chaotic and random vibration characteristic using a quarter vehicle model. Tusset *et al.* [7] investigated the performance of magnetorheological damper in quarter vehicle model using an intelligent controller.

In the longitudinal direction of the vehicle model, Jansen *et al.* [8] and Aparow *et al*. [9] studied on the ABS performance using quarter vehicle model. Furthermore, a regenerative braking system has been tested using a quarter vehicle model [10]. Meanwhile, there are other researchers whom mainly focus on the performance of the vehicle model in lateral direction. Rauh [11] examined both ride and handling performance by using a quarter vehicle model. Similarly, Zin *et al.* [12] developed simplified handling model known as 2 DOF bicycle model to evaluate the performance of vehicle in handling and suspension control. Meijaard and Schwab [13] investigated bicycle model to study on the handling performance due to the effect of a pneumatic trail and a damping at the tire contact. Baslamisli *et al.* [14] used bicycle model to develop active steering system using gain scheduled method.

Nevertheless, other researchers have enhanced the research scope to a higher degree of freedom such as Thompson and Pearce [15] examined the performance index for an optimal control for half vehicle active suspension by using the spectral decomposition method. Likewise, Gao *et al.* [16] also investigated the dynamic performance of vehicle under random road input excitations. Besides, a non-linear control integrated with active suspension is analysed on half vehicle model using road-adaptive algorithm [17]. Studies on quarter and half vehicle model have shown that the model is very useful in various applications. However, these models do not allow the automotive researchers to evaluate the vehicle model in lateral and longitudinal direction due to its limitation to include the steering, throttle and brake input from the driver. Thus, the researchers start to develop non-simplified vehicle model or known as a full vehicle model.

A lot of researches have been developed by previous researchers to analyze the performance of vehicle model in lateral, longitudinal and vertical direction. Ahmad *et al.* [18] have used 14-DOF vehicle ride model to develop active suspension using adaptive PID with pitch moment rejection control. Meanwhile, 14-DOF vehicle handling model has been used for active suspension system with roll moment rejection control [19]. Aparow *et al.* [20] also developed 5-DOF full vehicle model in longitudinal direction to study on ABS performance. Besides, Hudha *et al.* [21] also have examined the 12-DOF ride model of an armored vehicle by controlling the suspension system with effect from gun system and also road irregularities. Similarly, Trikande *et al.* [22] has studied 11 DOF armored vehicle on ride performance of the model using semi-active suspension due to the firing attack and instability of the vehicle. However, all the previous studies have analyzed the performance of the vehicle model only in one direction by neglecting other direction. It shows that the proposed vehicle model is applicable for a single testing procedure only. Moreover, the effect from steering inertia, effect of throttle torque from engine and also surrounding disturbance are mostly neglected while developing a full vehicle model.

In order to overcome this shortcomings, a combination of both lateral and longitudinal of vehicle model has been developed in this study. The developed vehicle model is mainly designed for armored type of vehicle whereby the system configuration of steering system is used based on Pitman arm system and the internal combustion engine is developed for the armored vehicle model with an additional gun turret system is mounted on to of the armored vehicle. Meanwhile, the hydraulic brake actuator model is used in this study to represent a simplified model of brake system dynamics from a physical modeling [20]. The three main inputs which are steering, throttling and braking from the driver are used during testing in both directions. The developed armored vehicle model is evaluated using validated CarSim software on both lateral and longitudinal direction. It demonstrates the capability of the developed vehicle model to be tested using more than single direction without adjusting the subsystems or parameters

This paper is organized as follows: The first section represents the introduction and review of some related works. The second section is followed by modeling the dynamic behavior of armored vehicle model in lateral and longitudinal direction by proposing Pajecka Magic formula as the tire model and the vehicle input models such as Pitman Arm steering system, powertrain and hydraulic assisted brake model of an armored vehicle dynamic model. The following section discusses the verification procedure using validated CarSim software and discuss about the performance of the armored vehicle model in lateral and longitudinal direction. The fifth section discusses the future work of proposed armored vehicle model and finally is the conclusion

2.0 A 9 DOF ARMORED VEHICLE MODEL

A 9 DOF of an armored vehicle considered in this study consists of a single sprung mass (vehicle body) connected to four unsprung masses. The vehicle model is developed by combining the lateral [23,24] and longitudinal dynamic [20, 25] of the vehicle model. Hence, this paper focuses on the performance of an armored vehicle model in both lateral and longitudinal directions. Each wheel is allowed to rotate along its axis and only the two front wheels are free to steer during cornering. The suspensions system between the sprung mass and unsprung masses is assumed to be ideal since the normal forces, F_z at each tire can be obtained using load distribution equilibrium motion. Besides, the aerodynamic drag force and rolling resistance due in the longitudinal direction to body flexibility are also considered in developing the 9 DOF vehicle model. Tire model behavior is modeled using the Pacejka Magic Tire Model [26] by considering the lateral and longitudinal forces and also self-aligning moment. The steering system is modeled as a 2 DOF motion using Pitman Arm steering equation. Power train and brake dynamics are included in the modeling as it contributes significantly in the performance of the vehicle model during cornering, accelerating and braking conditions

2.1 Load Distribution Model

As in Aparow *et al.* [20], Short *et al.* [25] and Ping *et al.* [27] the load distribution of a vehicle model can be developed using lateral acceleration, a_y and longitudinal acceleration, a_x as shown in Figure 1.

In this case, the dynamic load distribution is transferred between left and right wheels as the vehicle undergoes cornering condition. Meanwhile, the load between the front and rear wheels can be transferred as the vehicle is in accelerating and braking conditions. From the geometry, two equations can be formulated in order to describe the front and rear normal forces:

$$F_{z,fl/fr} = [\frac{mg}{2}(\frac{l_r}{t}\cos\theta + \frac{h}{t}\sin\theta)] \pm [ma_y(\frac{h}{t})(\frac{l_f}{l})] - [\frac{ma_x}{2}(\frac{h}{l})] \quad (1)$$

$$F_{z,rl/rr} = [\frac{mg}{2}(\frac{l_f}{t}\cos\theta + \frac{h}{t}\sin\theta)] \pm [ma_y(\frac{h}{t})(\frac{l_r}{l})] + [\frac{ma_x}{2}(\frac{h}{l})] \quad (2)$$

where l is the total length of the armored vehicle. Meanwhile, θ is the road gradient. In this study, the road profile is assumed a flat.

2.2 Pacejka Magic Tire Model

The behavior of the tire model plays very important role in controlling an armored vehicle in longitudinal and lateral directions. Therefore, a good representation of a tire behavior is a necessity in developing the vehicle model. The tires provide the longitudinal and lateral forces which affect the speed and direction of the armored vehicle while traveling on an uneven road profile. Several analytical tire models have been developed in order to analyze and simulate slip/friction characteristics. One of the tire model is the Pacejka Magic Formula Tire Model [26,28]. The Pacejka Magic Tire Model calculates the lateral force and aligning moment based on slip angle (in degree) and longitudinal force based on percentage of longitudinal slip. The Pacejka Tire model is derived mathematically for the four tires as below:

$$y_{fl/fr}(x_{fl/fr}) = D\sin\left[C\arctan\left(Bx_{fl/fr} - E\left(Bx_{fl/fr} - \arctan\left(Bx_{fl/fr}\right)\right)\right)\right]$$
$$y_{rl/rr}(x_{rl/rl}) = D\sin\left[C\arctan\left(Bx_{rl/rl} - E\left(Bx_{rl/rr} - \arctan\left(Bx_{rl/rr}\right)\right)\right)\right] \quad (3)$$

$$Y(X) = y(x) + S_v \quad (4)$$
$$x = X + S_h$$

where Y(X) represents the value of cornering force, self-aligning torque or braking force. Meanwhile, X denotes slip angle or skid where X is used as the input variable such as slip angle α (lateral direction) or slip ratio λ (longitudinal direction). The model parameters B, C, D, E, S_v, and S_h represent stiffness factor, shape factor, peak value, curvature factor, horizontal shift, and vertical shift respectively, and the general form of Magic Tire formula is shown in Figure 2:

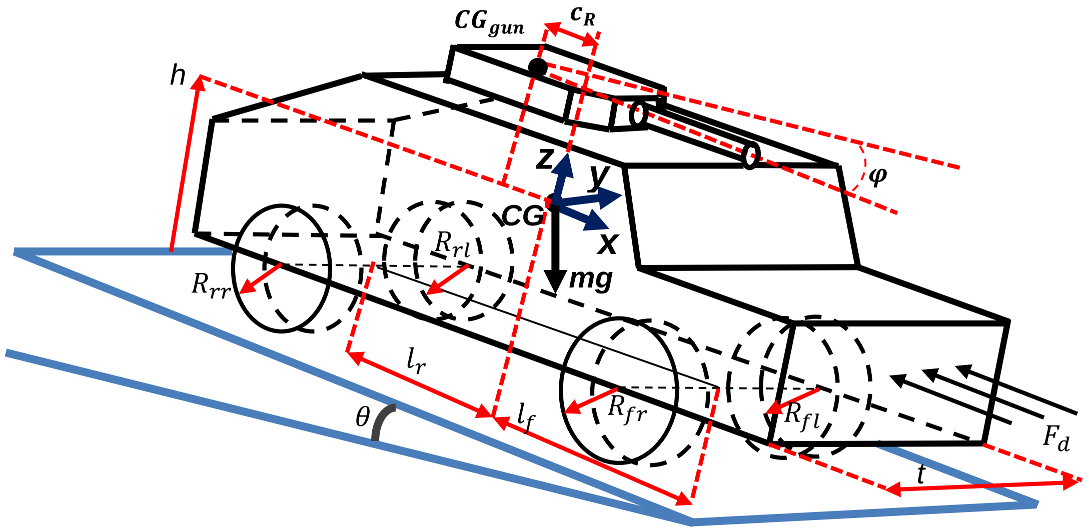

Figure 1 A 3D diagram of armored vehicle model

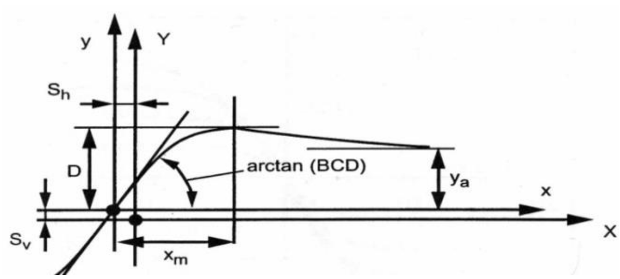

Figure 2 Characteristics of the Magic Formula tire test [25]

In order to define the model parameters *B, C, D, E,* S_v, and S_h for lateral force, self-aligning moment and longitudinal force, the equations are formulated as follows [28]. The equations are formulated using constant parameters a_1 to a_{11} and the constant parameters can be obtained from [28]. The responses of lateral force, self-aligning moment and longitudinal force are developed by referring to equation (5) to (14) using Matlab/SIMULINK. The responses are evaluated using four types of normal force, F_z which are 2, 4, 6 and 8 kN which indicating minimum to maximum normal force occurred on vehicle's tires.For the lateral force, the stiffness, shape, peak and curvature factors are calculated as follows:

$$BCD = a_3 \sin\left(a_4 \tan^{-1}(a_5 F_z)\right) \quad (5)$$
$$B = BCD/CD \quad (6)$$
$$D = a_1 F_z^2 + a_2 F_z \quad (7)$$
$$C = 1.30 \text{ (constant value)}$$
$$E = a_6 F_z^2 + a_7 F_z + a_8 \quad (8)$$

The factors are slightly affected by the camber angle, denotes as γ_c, in degree

$$S_h = a_9 \gamma_c \quad (9)$$

$$S_v = (a_{10} F_z^2 + a_{11} F_z)\,\gamma_c \quad (10)$$

The model for lateral force is analyzed using various constant normal force inputs to observe the behavior of the model and the response shows in Figure 3:

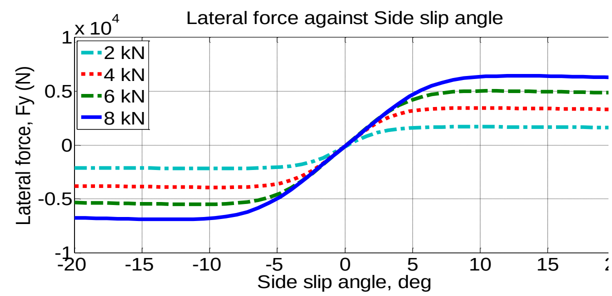

Figure 3 Lateral force against slip angle

For both self-aligning moment and longitudinal force, the stiffness, shape, peak and curvature factors are calculated as follows

$$BCD = (a_3 F_z^2 + a_4 F_z)/e^{a_5 F_z} \quad (11)$$
$$B = BCD/CD \quad (12)$$
$$D = a_1 F_z^2 + a_2 F_z \quad (13)$$
$$E = a_6 F_z^2 + a_7 F_z + a_8 \quad (14)$$

The constant value C for self-aligning moment is 2.40 and for longitudinal force is 1.65. Meanwhile, the value of S_h and S_v can be obtained from equation (10) and (11). The model for self-aligning moment and longitudinal force are analyzed using various constant normal force inputs to observe the behavior of the model and the response of self-aligning moment are shown in Figure 4 and longitudinal force in Figure 5 as follow:

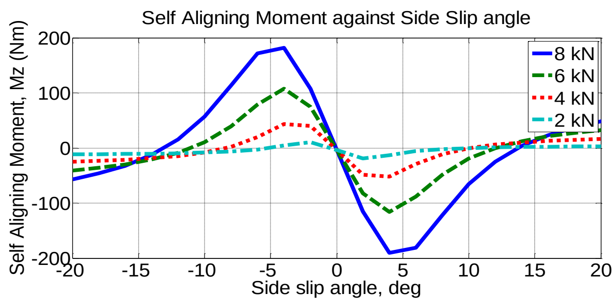

Figure 4 Self-aligning moment against slip angle

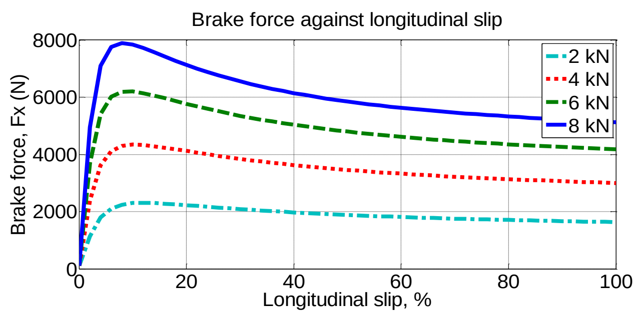

Figure 5 Longitudinal force against slip ratio

2.3 Handling Model

The handling model described in this paper is a 7 degrees of freedom system as shown in Figure 6. It consists of 3 degrees of freedom of the armored vehicle body in lateral and longitudinal motions as well as yaw motion (r) and a single degree of freedom due to the rotational motion of each tire. The armored vehicle experiences motion along the longitudinal x-axis, the lateral y-axis, and the angular motions of yaw around the vertical z-axis. The motion in the horizontal plane can be characterized by the longitudinal and lateral accelerations, denoted by a_x and a_y respectively. In order to obtain the lateral and longitudinal accelerations, summations of total forces acting in lateral and longitudinal directions are considered in this model. The total longitudinal forces acting at the front and rear of the armored vehicle is the sum of the normal, drag and recoil force as

$$F_{x_{total}} = ma_x$$
$$= F_{xrr} + F_{xrl} + F_{yfr}\sin\delta_f + F_{yfl}\sin\delta_f + F_{xfr}\cos\delta_f + F_{xfl}\cos\delta_f + mg\sin\theta - F_d + F_R\cos\varphi \qquad (15)$$

The F_R is the recoil force due to gun firing. The drag force, F_d, is an important in the model which is used to limit the maximum linear speed of a vehicle in the longitudinal direction. The drag force can be derived by summing the aerodynamic resistance force, F_a and rolling resistance force, F_r as shown below:

$$F_d = F_a + F_r = \frac{1}{2}\rho A C_d(v_x^2) + mgC_r(v_x) \qquad (16)$$

Since the armored vehicle model is developed based on both lateral and longitudinal dynamics, hence the equation related to drag force acting in the longitudinal direction is summed as the total of forces acting in the longitudinal direction in order to obtain longitudinal acceleration, a_x. Meanwhile, the total force acting in the lateral direction is

$$F_{y_{total}} = ma_y$$
$$= F_{yrr} + F_{yrl} + F_{yfr}\cos\delta_f + F_{yfl}\cos\delta_f - F_{xfr}\sin\delta_f - F_{xfl}\sin\delta_f - F_R\sin\varphi \qquad (17)$$

The yaw acceleration, $\dot{r}$, is also dependent on the longitudinal and lateral forces, F_x and F_y which are acting on each of the front and rear tires. Besides, the self-aligning moment from each tires are also considered in deriving the total yaw moment acting at CG of the vehicle, thus

$$M_{yaw} = I_{yaw}\dot{r}$$
$$= [F_{xrr} - F_{xrl} - F_{yfr}\sin\delta_f + F_{yfl}\sin\delta_f - F_{xfr}\cos\delta_f + F_{xfl}\cos\delta_f]\,t/2 + [F_{yrr} + F_{yrl}]l_r + [-F_{yfr}\cos\delta_f - F_{yfl}\cos\delta_f + F_{xfr}\sin\delta_f + F_{xfl}\sin\delta_f]l_f + M_{z_{fl}} + M_{z_{fr}} + M_{z_{rl}} + M_{z_{rr}} + [(F_R\sin\varphi)\times c_R] \qquad (18)$$

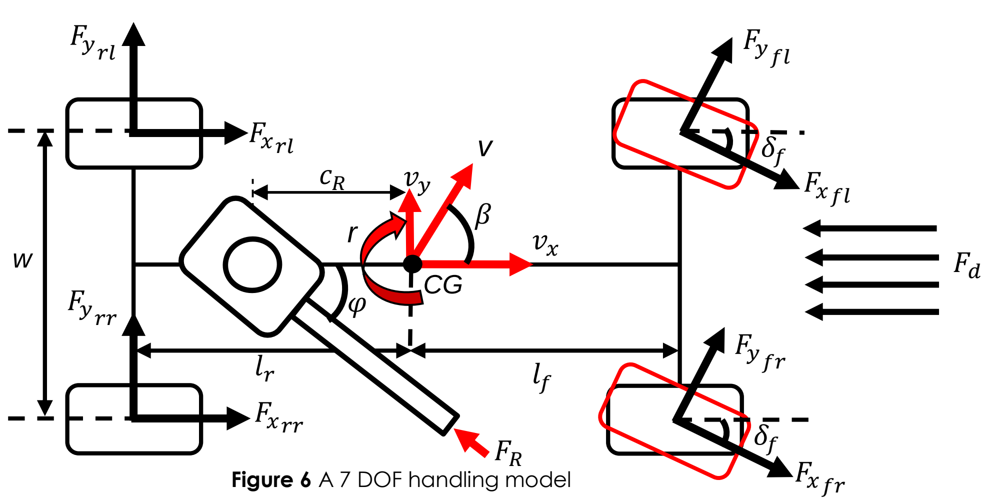

Figure 6 A 7 DOF handling model

To complete the handling model, the summation of torques acting about each wheel needs to be included. Based on the summation of the torque of the wheels, the rotational velocity, ω, of the wheel can be obtained as

$$(I_{fi,j} \times \dot{\omega}_{fi,j}) = \tau_{e_{fi,j}} + \tau_{r_{fi,j}} - \tau_{b_{fi,j}} - \tau_{d_{fi,j}}(\omega_{fi,j})$$
$$(I_{ri,j} \times \dot{\omega}_{ri,j}) = \tau_{r_{ri,j}} - \tau_{b_{ri,j}} - \tau_{d_{ri,j}}(\omega_{ri,j}) \qquad (19)$$

where $\tau_{e_{fl/fr}}$ are the torques delivered by the engine to each front wheels only since a front wheel drive vehicle is assumed and the rear wheel is assumed to be zero. Meanwhile, $\tau_{b_{fl/fr}}$ and $\tau_{b_{rl/rr}}$ are the brake torques applied to each front and rear wheels during braking input. The engine model will be discussed in the following sections. The reaction torques which are $\tau_{r_{fl/fr}}$ and $\tau_{r_{rl/rr}}$, occurred on each front and rear wheels because of tire traction force. A detailed derivation of summation of torques in wheel can be obtained from Aparow *et al.* [20].

The lateral and longitudinal acceleration are influenced by the yaw response acting at CoG of the armored vehicle. Hence, the lateral and longitudinal acceleration response obtained from the equation (15) and (17) is derived by considering the effect from yaw motion given by

$$\dot{v}_x = a_x + v_y\dot{r} \qquad (20)$$
$$\dot{v}_y = a_y + v_x\dot{r} \qquad (21)$$

The longitudinal and lateral velocities of vehicle can be obtained by integrating equations (22) and (23). Body velocities can be used to identify the armored vehicle body side slip angle, denotes by β:

$$\beta = \tan^{-1}\left[\frac{v_y}{v_x}\right] \qquad (22)$$

2.4 Longitudinal and Lateral Slip Model

The longitudinal and lateral velocities of the armored vehicle can be obtained from equations (20) and (21) by integrating $\dot{v}_x$ and $\dot{v}_y$ respectively. It can be used to obtain the tire lateral slip angle, denoted by α. Thus, the tire lateral slip angle at front and rear tires can be derived as:

$$\alpha_{fl/fr} = \tan^{-1}\left[\frac{v_y + l_f\dot{r}}{v_x + (\frac{t}{2})\dot{r}}\right] - \delta_f$$
$$\alpha_{rl/rr} = \tan^{-1}\left[\frac{v_y - l_r\dot{r}}{v_x + (\frac{t}{2})\dot{r}}\right] \qquad (23)$$

where, α_f and α_r are the lateral slip angles of tires at the front and rear of the vehicle. The wheel angle, δ_f, affects the front lateral slip angle, α, only since only the front wheel is steered via steering input. The longitudinal slip, λ, known as the effective coefficient of force transfer, is obtained by measuring the difference between lthe longitudinal velocity of the vehicle, v_x, and the rolling speed of the tire, ωR, where R_w represents the radius each wheel [20].

2.5 Development of Lateral and Longitudinal Input Models

Three types of input models are developed in this study to define the direction of the armored vehicle either in lateral or longitudinal motion. The inputs are categorized as steering, powertrain and brake input models. In order to investigate the performance of the 9 DOF vehicle model in lateral and longitudinal directions, few assumptions need to be considered. For the lateral condition, the vehicle is assumed to travel with constant engine torque and longitudinal velocity without brake input. Meanwhile, for the longitudinal condition, the vehicle is assumed to move in a straight direction without any steering input from the driver. All three inputs are described in this section.

2.5.1 Two DOF Pitman Arm Steering Model

There are two types of steering system commonly used in vehicles which are rack and pinion steering system and Pitman arm steering. Generally, rack and pinion steering is used in a passenger vehicle meanwhile a Pitman arm steering is used in a armored vehicle. Since this study focuses on armored vehicle, a 2 DOF hydraulic powered Pitman arm steering model is developed based on the system as shown in Figure 7. The 2 DOF represents the rotational motion of steering column and translational displacement of steering linkage. There are four main equations in developing Pitman Arm Steering equation which are:

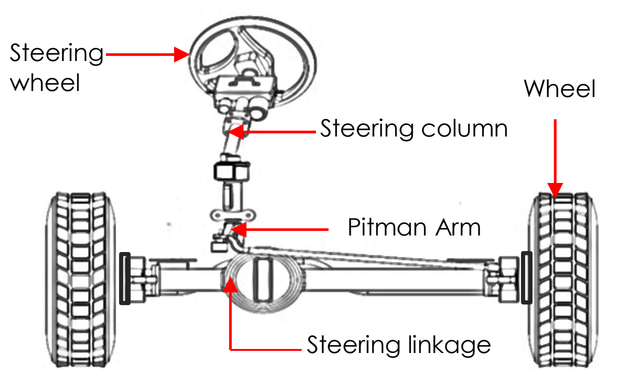

Figure 7 Pitman arm steering system

Steering Wheel Equation

The steering wheel is connected to the steering column as shown in Figure 8 and the response is obtained as follows [29]:

$$J_{sw}\ddot{\theta}_{sw} + B_{sw}\dot{\theta}_{sw} + K_{sc}(\theta_{sw} - \theta_{sc}) = T_{sw} \qquad (24)$$

where T_{sw} is torque at steering wheel, θ_{sc} and θ_{sw} is angular displacement of steering column and steering wheel.

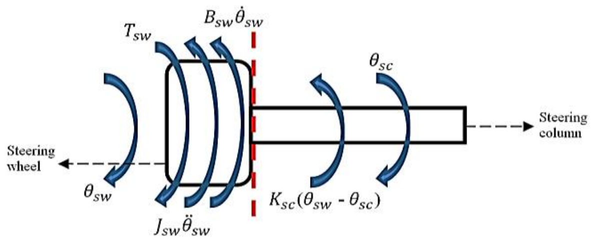

Figure 8 Steering wheel and column

Steering Column Equation

In order to develop steering column equation, a few parts in the mechanisms need to be considered in the equation which is steering column itself, universal joint, hydraulic assisted pump, worm gear, sector gear and Pitman Arm. Since this is a conventional Pitman Arm steering for a armored vehicle, the torque of DC motor is neglected in this study. The equation of steering column is given by:

$$J_{sc}\ddot{\theta_k} + B_{sc}\dot{\theta_k} + K_{sc}(\theta_k - \theta_{sw}) = T_{HP} - T_{PA} - F_C \text{ sign } \dot{\theta_k} \quad (25)$$

where T_{HP} and T_{PA} are the torque due to Hydraulic Assisted Pump and at Pitman Arm Steering, F_c is Steering Column friction. Due to the limitation of space at engine location of the armored vehicle, the hydraulic power assisted system cannot be located at the same axis as the steering wheel. Hence, an additional join known as universal joint is used as solution to overcome the space constraint. A universal joint allows transmission of torque occurred between two nonlinear axes. This introduces slight deviation in angle as shown in Figure 9 which is referred as ∅ between two axes [30,31].

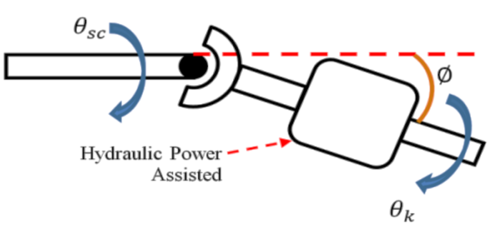

Figure 9 Universal Joint at steering column

The universal joint angle is used for the steering mechanism since it is a flexible coupling where it is rigid in torsion but compliant in bending. The angle of ∅ is set at 20 degree lower than the steering column, θ_{sc} [32]. The angle θ_k is described as:

$$\theta_k = \tan^{-1}(\tan\theta_{sc}/\cos\emptyset) \quad (26)$$

The other mechanism connected to the steering column is the hydraulic power assisted unit. This unit enables elimination of extensive modifications to the existing steering system and reduces effort by the driver to rotate the steering wheel since the hydraulic power assisted unit is able to produce large steering effort using hydraulic pump, rotary spool valve and Pitman arm. The rotary spool valve consists of torsion bar, inner spool and also outer sleeve. Once input is given to the steering wheel, it produces torque to twist the torsion bar and it rotates the inner spool with respect to the outer sleeve. This rotation tends to open the metering orifices hence increases the hydraulic fluid flow to actuate the worm gear. The hydraulic fluid flow through an orifice can be described as:

$$Q_o = A_o \times C_{do}\sqrt{2\Delta P/\rho} \quad (27)$$

where A_o is cross sectional area of the orifice and ΔP is differential pressure across the orifice. The overall hydraulic power assisted equation can be derived by applying equation (30) by using the metering orifices, rotary spool valve and also applying the mass conservation method to obtain the following equations [30]:

$$Q_s + A_1C_d\sqrt{2/\rho\sqrt{|P_s - P_r|}} = (V_s/\beta_f)\dot{P_s} \quad (28)$$

$$A_1C_d\sqrt{2/\rho\sqrt{|P_s - P_r|}} - A_2C_d\sqrt{2/\rho\sqrt{|P_r - P_o|}} - A_P\dot{y}_L = \left(A_p\left((L/2) + y_r\right)/\beta_f\right)\dot{P_r} \quad (29)$$

$$A_2C_d\sqrt{2/\rho\sqrt{|P_s - P_l|}} - A_1C_d\sqrt{2/\rho\sqrt{|P_l - P_o|}} + A_P\dot{y}_L = \left(A_p\left((L/2) - y_r\right)/\beta_f\right)\dot{P_l} \quad (30)$$

Thus, the torque produced by the hydraulic power assisted can be obtained by the net force on the piston due to the pressure difference multiplied by steering arm length, l_s,

$$T_{HP} = l_s \times A_p \times (P_l - P_r) \quad (31)$$

where P_s is pump pressure, P_r and P_l are the right and left cylinder pressure. The output from the hydraulic power assisted model is connected to the worm gear where this gear is directly connected to the sector gear and attached to a member link called Pitman Arm. The Pitman Arm converts the rotational motion of the steering column into translational motion at the steering linkage. The configuration of worm gear, sector gear and Pitman Arm member is shown in Figure 10. Based on Figure 10, the output torque of the pitman arm link, τ_{PA}, can be obtained by equating both worm and sector gear as:

$$\tau_{wg} = K_{tr}(\theta_k - \theta_{wg}) \quad (32)$$

$$\tau_{sg} = \eta_{sg} \times \tau_{wg} \quad (33)$$

Since the torque created at sector gear is equal to the torque created at the end joint of pitman arm,

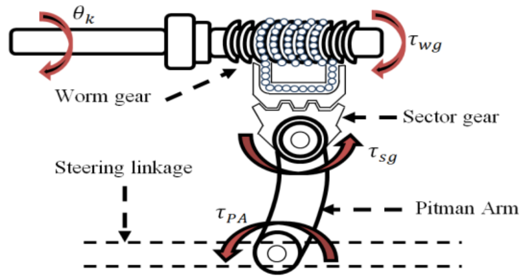

Figure 10 Mechanical configuration between worm gear, sector gear and pitman arm

$$\tau_{sg} = \tau_{PA} \tag{34}$$

where τ_{sg}, τ_{wg} and τ_{PA} are the torques at sector gear, worm gear and at pitman arm joint.

Steering Linkage Equation

The rotational input from the sector gear is converted into translational motion to the steering linkage using Pitman Arm joint link. By using the torque from Pitman Arm as the input torque, the equation of motion of the steering linkage is [29]:

$$M_L\ddot{y}_L + B_L\dot{y}_L + [C_{SL}\ \text{sgn}\ (\dot{y}_L)] - [\frac{b_r \times T_{PA}}{M_L \times R_{PA}}] = \eta_f(\frac{T_{PA}}{R_{PA}}) - \eta_B(\frac{T_{KL}}{N_M}) \tag{35}$$

and torque at steering linkage, T_{KL} is

$$T_{KL} = K_{SL}\ (\frac{y_L}{N_M} - \delta_f) \tag{36}$$

where M_L is the Mass of steering linkage of Pitman Arm Steering, B_L and y_L are viscous damping and translational displacement of steering linkage and b_r is resistance occurred on steering linkage. R_{PA} is radius of Pitman Arm and N_M is the motor gearbox ratio.

Equation of Motion of Wheel

Using equations (24), (25), (31) and (35), equation of motion of the wheel can be obtained. The output response of wheel equation of motion, known as wheel angle, δ_f, is given by

$$J_{fw}\ddot{\delta}_f + B_{fw}\dot{\delta}_f + [C_{fw}\text{sign}\ (\dot{\delta}_f)] = T_{KL} + T_{ext} + T_a \tag{37}$$

where J_{fw} is moment of Inertia of wheel, B_{fw} is viscous damping of steering linkage bushing, C_{FW} is coulomb friction breakout force on road front wheel, T_{ext} is external torque due to road wheel and T_a is tire alignment moment from Pacejka Magic Tire model. The front wheel angle, δ_f, obtained from the 2 DOF Pitman arm steering model is used in equations (15), (17), (18) and (23).

2.5.1 Power Train Model

The powertrain model is one of the important subsystems in the vehicle model to generate engine torque in order to produce rotational motion to the front wheels. The model consists of internal engine dynamics, gearbox and final drive differential model. These models are used to transfer the engine torque to the front wheels once the vehicle starts to accelerate, cornering or braking [20, 25].

Engine Dynamics

The engine dynamics have been developed based on Moskwa and Hedrick [33] which focuses on automotive engine meanwhile Wahlström and Eriksson [34] focused on diesel type of engine. The equations developed are more focused with three variables which are mass of air intake manifold, engine speed, mass flow rate of fuel entering combustion chamber and the output torque. By applying the law of conservation of mass to the air flow in the intake manifold, the following equation can be obtained:

$$\dot{m}_a = \dot{m}_{ai} - \dot{m}_{ao} \tag{38}$$

and

$$\dot{m}_{ai} = MAX \times TC \times PRI \tag{39}$$

where m_a is mass of air in the intake manifold, $\dot{m}_a$, $\dot{m}_{ai}$, are the mass rate of air in the intake manifold, mass rate of air entering the intake manifold. $\dot{m}_{ao}$ is leaving the intake manifold and entering the combustion chamber. Meanwhile, TC is the normalized throttle characteristic and PRI is. The term TC can be determined based on experimental data as shown by Moskwa and Hedrick [33]. The data is described as below:

$$TC = \begin{cases} 1 - \cos[(1.14459 \times \alpha_t) - 1.06]; & \alpha_t \leq 79.5 \\ 1 & \alpha_t > 79.6 \end{cases} \tag{40}$$

where α_t is the throttle angle of the opening throttle body valve. Meanwhile, the normalized pressure influence function, *PRI*, is the normalized pressure influence function and measured as a ratio of function manifold to atmospheric pressure:

$$PRI = 1 - \exp[(P_m/P_{atm}) - 1] \tag{41}$$

The mass of air and also the intake manifold pressure enters the intake manifold is described using ideal gas law which is:

$$m_a = ((M_a \times P_m \times V_m)/(R \times T_m)) \tag{42}$$

Besides that, the flowing air from intake manifold to the combustion chamber is given by

$$\dot{m}_{ao} = h_{ve} \times \omega_e \times \eta_{vol} \times m_a \tag{43}$$

and h_{ve} is given as

$$h_{ve} = V_e/(4\pi \times V_m) \quad (44)$$

where P_m and P_{atm} are the intake manifold pressure and atmospheric pressure and ω_e is the engine angular velocity. The volumetric efficiency, η_{vol}, is used to represent the efficiency of the engine's initiation process. The volumetric efficiency is developed as a second order polynomial based on an experimental data [33], i.e.

$$\eta_{vol} = ((24.5 \times \omega_e) - 4.1 \times 10^4)m_a^2 + ((-0.167 \times \omega_e) - 350)m_a + ((8.1 \times 10^4) \times \omega_e) + 0.352) \quad (45)$$

Meanwhile, the dynamics of the field injection process can be described as below:

$$(r_f \times \ddot{m}_{fi}) + m_{fi} = \dot{m}_{fc} \quad (46)$$

where, the effective fueling time constant, r_f can be described as:

$$[(\dot{m}_{fc} \times \beta_{fc})/MAX] \times [1.5 \times \pi/\omega_e] - 0.025 = r_f \quad (47)$$

The term m_{fi} is the fuel rate entering the combustion chamber, $\dot{m}_{fc}$ is command fuel rate and β_{fc} is the desired air/fuel ratio [34]. By applying Newton's second law to the rotational dynamics of the engine, the third variable equation can be derived as:

$$(I_e \times \dot{\omega}_e) + T_{at} + T_{ft} = T_{it} \quad (48)$$

where T_{at} is known as accessories torque, T_{ft} is the engine friction torque, T_{it} is the engine indicated torque and I_e is the effective inertia of the engine. Generally, the process of torque generation is discrete where it depends on the rotational speed of the engine of a four stroke engine. Since the model developed is in a continuous state, two delays which are the T_{ft} and T_{it} are used to develop the equation. The indicated and friction torque, T_{ft} and T_{it}, which describes for the fuel injection type of engine for heavy vehicle such as armored vehicle can be referred from [34]. The throttle is assumed actuated by a servo by relating with time delay, t_{es}, which is lumped together into a single equivalent delay [20, 25] The time delay, t_{es} has been used to define the energy transfer co-efficient, μ_e.

$$\dot{\mu}_e = (((0.01\mu_t) - \mu_e)/t_{es}) \quad (49)$$

where μ_t is the input throttle setting (%). By defining an energy transfer co-efficient, μ_e which governs the actual torque response as a function of T_{it}, the front wheels torque of the armored vehicle is given by

$$\tau_{e_{fl/fr}} = \mu_e \times \eta_g \times \eta_f \times T_{it} \quad (50)$$

and η_g is the gear ratio (1st, 2nd, 3rd, 4th, 5th) and η_f is the final drive ratio.

Gearbox Model

An automatic transmission gearbox is used in this study by using shift logic system. The shift logic will produce mapping that relates the threshold for changing each gear up or down as a function of throttle setting and wheel speed [20]. The shift logic shows two conditions which are the throttle acceleration and deceleration. Figure 11 shows the shift logic graph for the gearbox model. The detail explanations of the shift up and down gear mapping can be obtained in Aparow *et al.* [20].

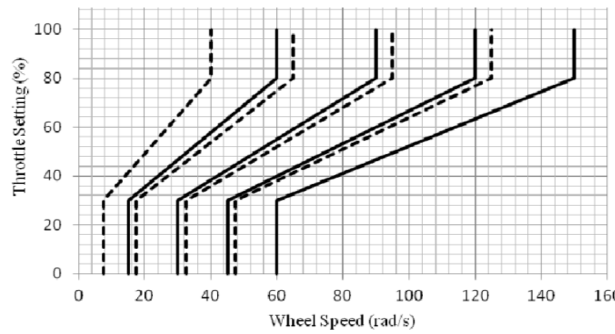

Figure 11 Automatic transmission gearbox shift logic [20]

2.5.3 Hydraulic Brake Model

The hydraulic brake dynamics is modeled as a first order linear system in conjunction with a pure time delay [35]. The vacuum power assist is represented as a two-state model and the remaining components such as brake hydraulics are modelled as nonlinear model. The detail derivation on the hydraulic brake model can be found in Aparow *et al.* [20].

2.6 9 DOF Lateral and Longitudinal Model

The armored vehicle model describing lateral and longitudinal motions was developed based on the mathematical equations derived in Sections 2.1 to 2.5 and simulated using MATLAB SIMULINK software. The relationship between pitman arm steering model, power train model, braking model, handling model, lateral and longitudinal slip model, Pacejka Magic tire model, wheel dynamic model and the load distribution model are clearly shown in Figure 12. Three types of inputs used are steering model input (angle), throttle setting (0-100%) and brake setting (0-100%). The model is able to be used for dynamic analysis of the vehicle in lateral and longitudinal directions. The parameter of the vehicle, engine and steering model are included in the Tables 1, 2 and 3 as shown in the appendix section.

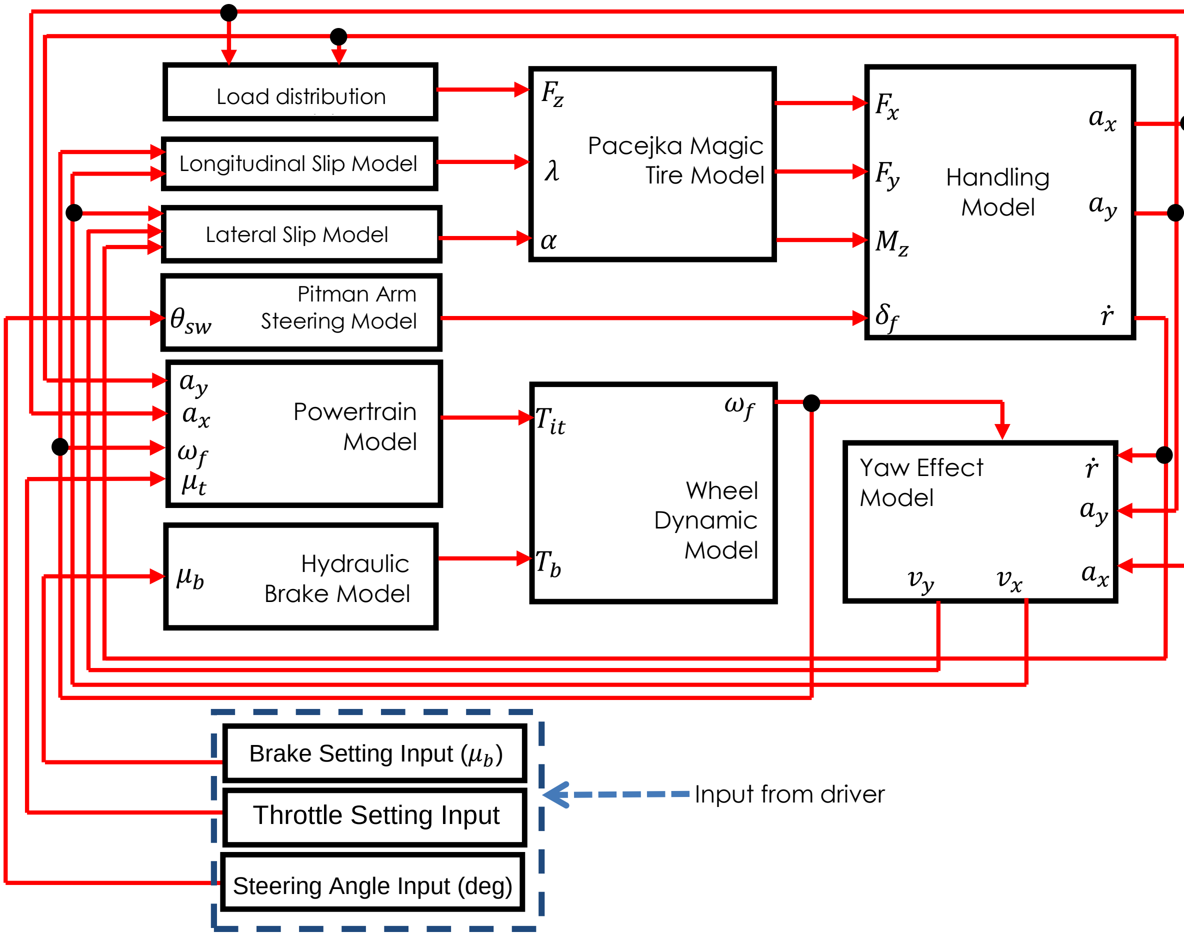

Figure 12 A 9 DOF armored vehicle model

3.0 VERIFICATION OF THE 9 DOF LATERAL AND LONGITUDINAL MODEL

In order to analyze the performance of the developed 9 DOF armored vehicle model, the response of the lateral and longitudinal motions of the model is compared with a validated vehicle simulator known as CarSim software. In this section, verification of the lateral and longitudinal vehicle model using visual technique is used by simply comparing the trend of simulation results between Matlab SIMULINK with the validated vehicle software where same type of inputs signals are used.

Verification procedure mainly refers as the comparison of developed model's performance with a validated or actual system. Hence, verification does not concern on fitting the simulated data exactly with the validated or actual system but used to obtain confident level that the developed simulation model shows similar behavior as an actual system. Therefore, model verification also can be defined as identifying the acceptability of a simulation model. It can be identified by using statistical tests on the deviation measure or qualitatively using visual techniques [21,23].

3.1 Verification Procedures

The dynamic behaviors considered in the lateral direction are the yaw rate, lateral acceleration, vehicle side slip angle, and tire side slip at each four tires. Meanwhile, dynamic behaviors considered in the longitudinal direction are longitudinal velocity, wheel velocity and longitudinal slip at each wheel and also the distance travelled by the vehicle. For the lateral condition, three types of test procedures are used such as double lane change, slalom and step steer test. For longitudinal motion, sudden acceleration and braking testing is used with three types of input conditions such as quarter, half and full throttle inputs. Hence, the validated software, CarSim 8.02, was configured to verify the 9 DOF armored vehicle model in lateral and longitudinal direction. An armored vehicle model, HMMWV (*available in CarSim*) is used in this study as the reference model. The parameters for the vehicle model which is used in Matlab Simulink are the same as the CarSim simulator. The input parameters for the verification procedure are listed in the Tables 1, 2 and 3. All the results are illustrated and discussed in the following sections using root mean square (RMS) error analysis.

3.2 Verification Results in the Lateral Direction

The verification procedure is initiated with the double lane change then followed by slalom and step steer test at 60 degrees angle input from steering wheel and each procedure tested at constant speed of 40 and 80 km/h. The steering inputs for each procedure are shown in Figures 13(a), 14(a) and 15(a) which are obtained from CarSim simulator. The armored vehicle model is verified in term of yaw rate, lateral acceleration, vehicle side slip and tires side slip. Each of the results are analysed in term of the root mean square (RMS) value of both simulation and validated CarSim data and measure the percentage of errors. The acceptable error range for the verification results are from 0% - 15% [36-38]. Figures 13(b) to 13(h) show the comparison of the results between CarSim data and simulation model using Matlab/SIMULINK for double lane change test for 40 and 80 km/h. It can be observed that trends between simulation and validated CarSim data are almost similar with acceptable error. The small deviation in magnitude occurred in the verification results since the data used in Carsim model are predicted based on the performance of vehicles in response to driver controls (steering, throttle, brakes, clutch, and shifting) with additional environment effects (road geometry, coefficients of friction, wind) compared to the proposed 9 DOF armored vehicle model by neglecting the effect of the ride and roll bar. Principally, the ride performance gives important role in minimizing the effect in vertical, pitch and roll response of the armored vehicle. However, the ride performance is neglected in this study since the suspension travel is not considered where a flat road surface has been used throughout the simulation. The percentages of errors show minor deviation in order to obtain similar trend results without implementing the ride model effect in the vehicle model.

Based on the results obtained in term of yaw rate, lateral acceleration and vehicle body slip angle, reasonable comparison is obtained by using double lane change condition as shown in Figures 13 (b), 13 (c) and 13 (d). The percentage of RMS errors for all three results at 40 km/h are 4.55%, 5.65%, 9.67% and 80 km/h are 4.6%, 5.6%, 11.1% respectively where the errors are less than 15%. Meanwhile, the response of tire side slip angle also shows a reasonable comparison with only some deviation up to 11.41% during maneuvering phase as shown in Figures 13(e), 13(f), 13(g) and 13(h). The slight deviation of the side slip angle occurred in each tire for both 40 and 80 km/h due to the roll effect which is neglected in the simulation model. However, the RMS errors obtained throughout the verification procedure are still below the acceptable range of error. Since the inertia of pitman arm steering is included in the simulation model, it has increased the degree of similarity of the armored vehicle model compare to the CarSim data in term of the trend and magnitude.

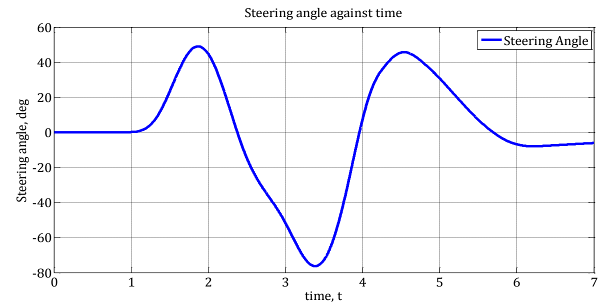

(a) Steering input against time

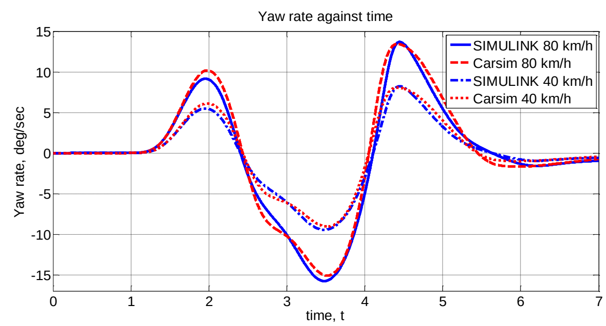

(b) Yaw rate against time

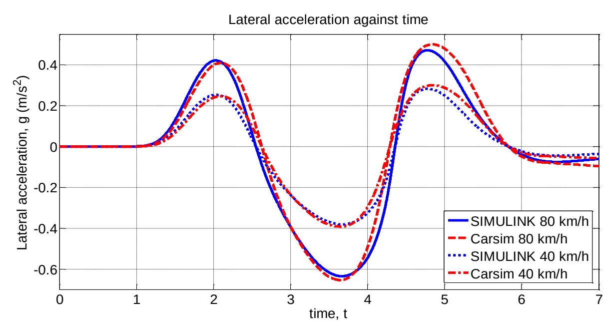

(c) Lateral acceleration against time

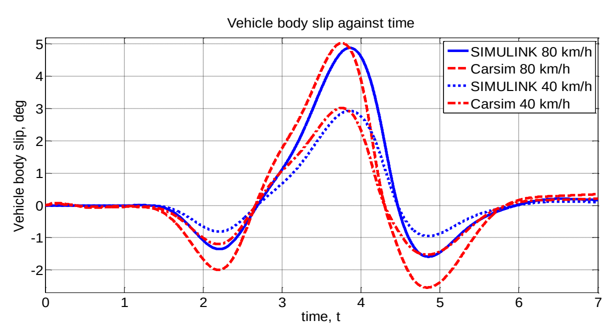

(d) Vehicle body slip against time

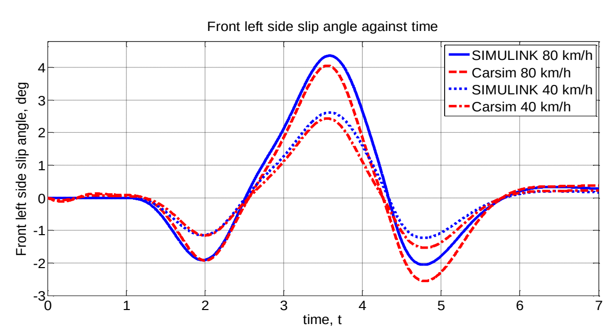

(e) Side slip Front left against time

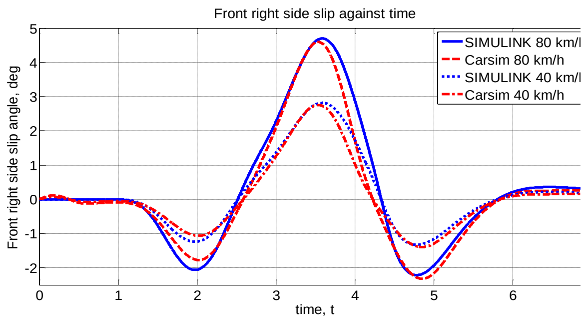

(f) Side slip Front right against time

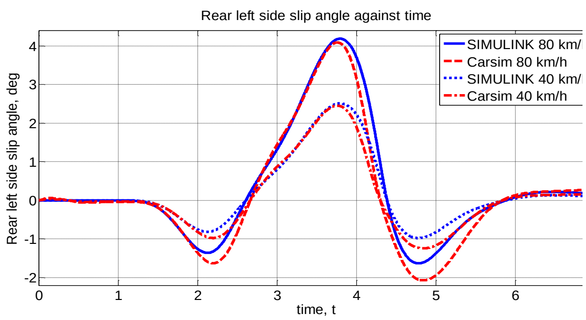

(g) Side slip Rear left against time

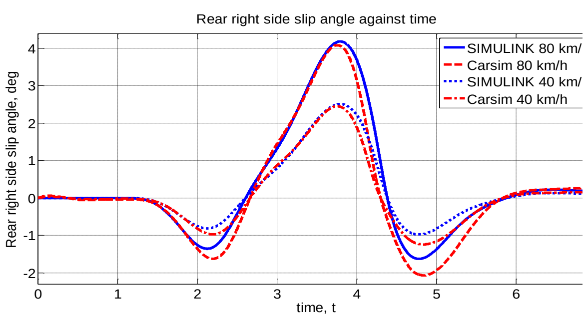

(h) Side slip Rear right against time

Figure 13 Response of the armored vehicle for double lane change test at 40 and 80 km/h

The test results of the slalom test at 40 and 80 km/h indicate that the simulation results and CarSim simulator relatively in good agreement as shown Figures 14(b) to 14(h). Figure 14(a) shows the steering wheel input from CarSim data used as the input for the simulation model during slalom test. In terms of yaw rate, lateral acceleration and vehicle body slip angle, it can be seen clearly that the simulation model results follow the CarSim data with some deviation in trend and also the magnitude as described in Figures 14(b), 14(c) and 14(d). Based on these results, the trends between simulation results and CarSim simulator data are having similar response with maximum error up to 8.2% based on RMS analysis.

This small fluctuation occurred in the CarSim data may be due to the flexibility of the vehicle body which was neglected in the simulation model. Nevertheless, by considering the pitman arm steering model which is supported by hydraulic power assisted unit in the simulation model has improved the performance of simulated vehicle model compared to CarSim data. The reduction of the deviation RMS errors can be observed in the responses of the tire side slip angles as shown in Figure 14(e), 14(f), 14(g) and 14(h). The responses show small differences between simulation and CarSim data with maximum percentage RMS error up to 8.9 % even though the ride and anti-roll bar effect is ignored in this simulation model. The overall percentage errors of the RMS value for each results are given in Table 4.

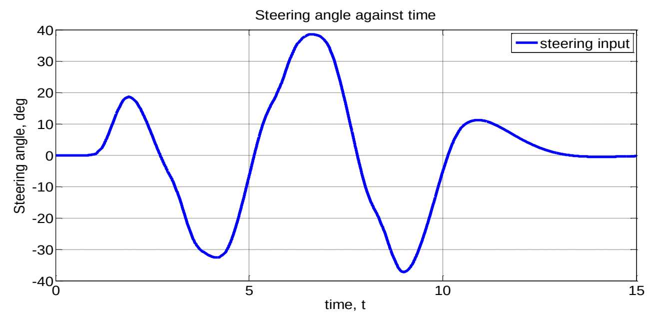

(a) Steering input against time

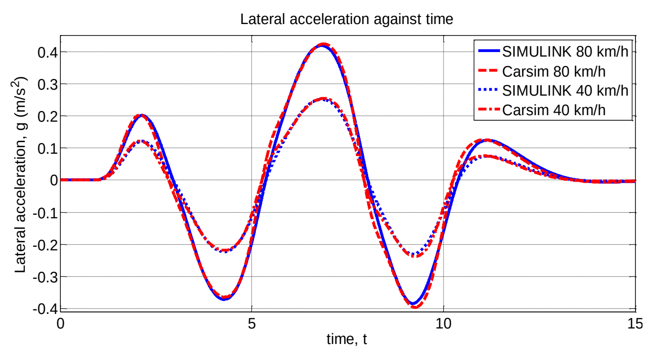

(b) Lateral acceleration against time

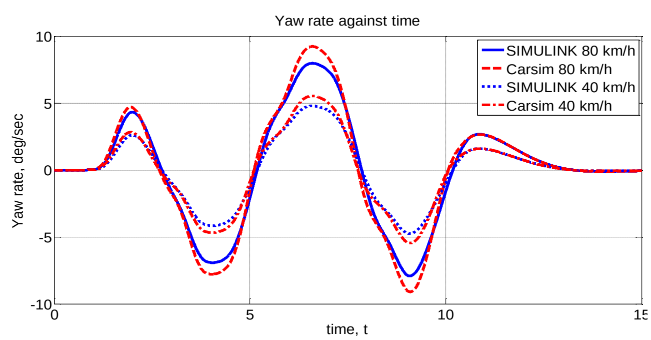

(c)Yaw rate against time

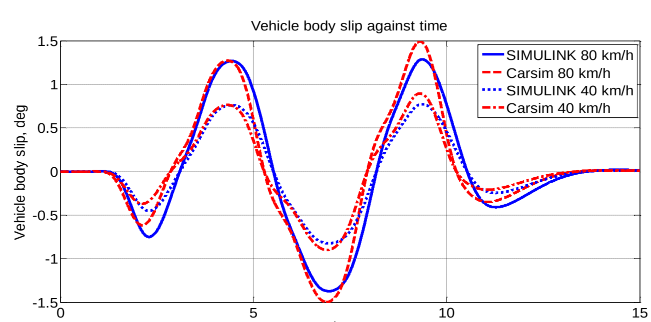

(d) Vehicle body slip against time

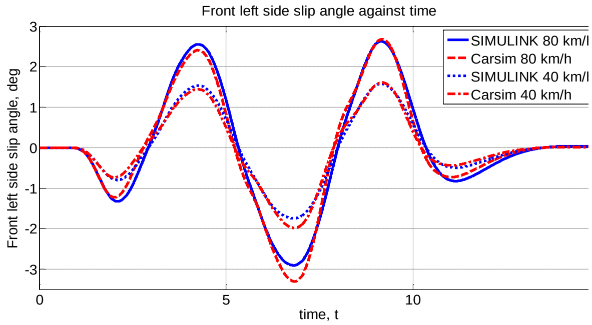

(e) Front left slip angle against time

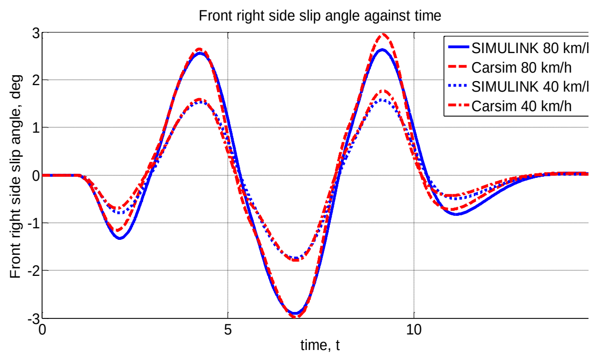

(f) Front right slip angle against time

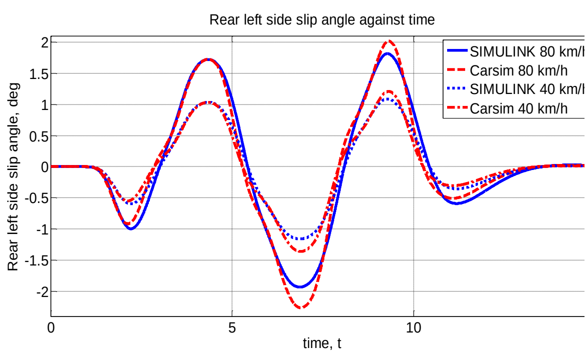

(g) Rear left slip angle against time

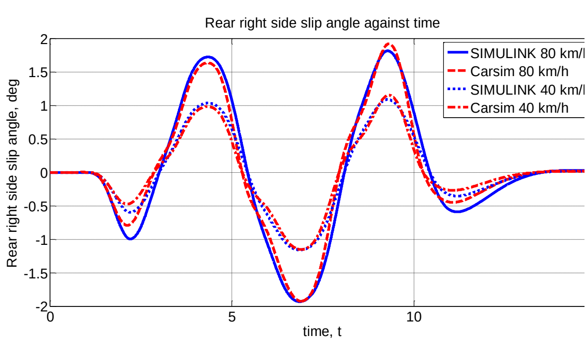

(h) Rear right slip angle against time

Figure 14 Response of the armored vehicle for slalom test at 40 km/h and 80 km/h

Similarly, the response of the step steer at 60 degree turn angle procedure at 40 and 80 km/h also shows comparable behavior between simulation model and CarSim data as shown in Figure 15. Based on the results obtained in term of the yaw rate, lateral acceleration and also vehicle body slip angle, a reasonable comparison is obtained during the initial transient phase as well as steady state phase as shown in Figures 15(b), 15(c) and 15(d). It can be seen that the behavior of the simulation model and CarSim data are almost similar with acceptable RMS error. The percentages of RMS errors for lateral acceleration, yaw rate and vehicle body slip at 40 km/h are 0.4%, 5.2%, 2.3% and at 80 km/h are 0.4%, 4.8% and 2.7%, respectively. Meanwhile, the tire side slip angle response shows satisfactory trend with a small deviation during the transition area between steady state phase and the transient phase as shown in Figures 15(e), 15(f), 15(g) and 15(h). The percentage of RMS errors for tire side slip angles are 9.0%, 9.1%, 2.5% and 2.1% respectively. Henceforth, it can be concluded that simulation model in the lateral direction have similar behavior as the CarSim data with minor acceptable RMS error. The following section describes the performance of the simulation model compared with CarSim data in the longitudinal direction.

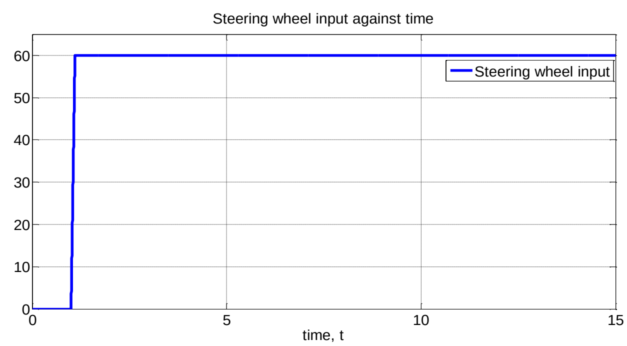

(a) Steering input against time

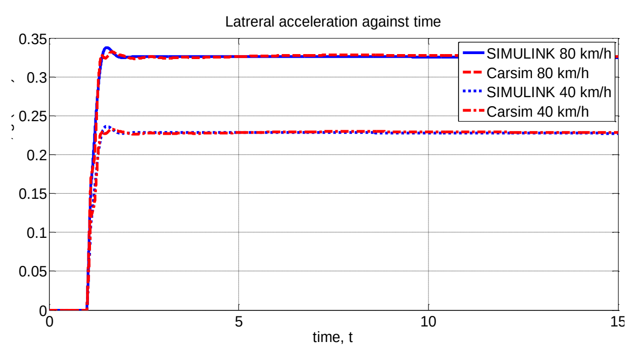

(b) Lateral acceleration against time

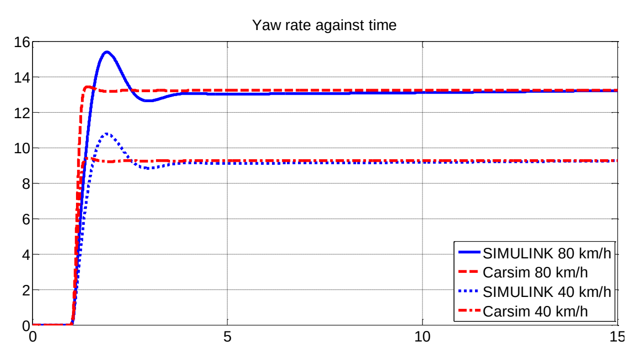

(c) Yaw rate against time

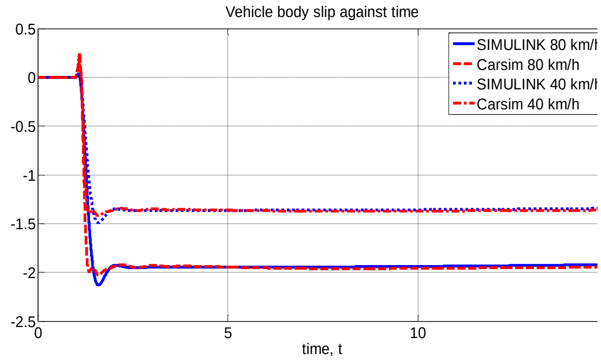

(d) Vehicle body slip against time

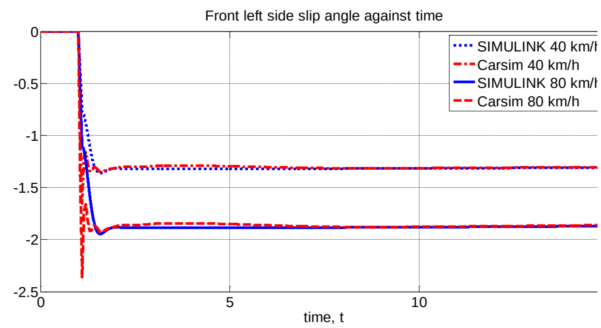

(e) Front left slip angle against time

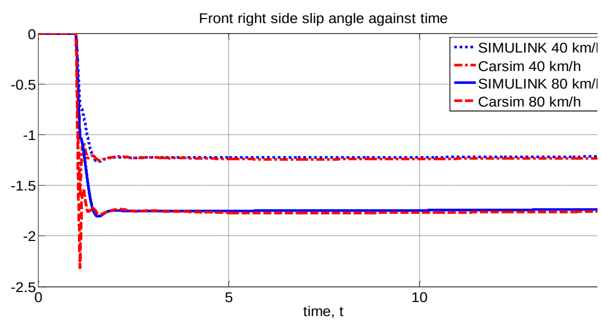

(f) Front right slip angle against time

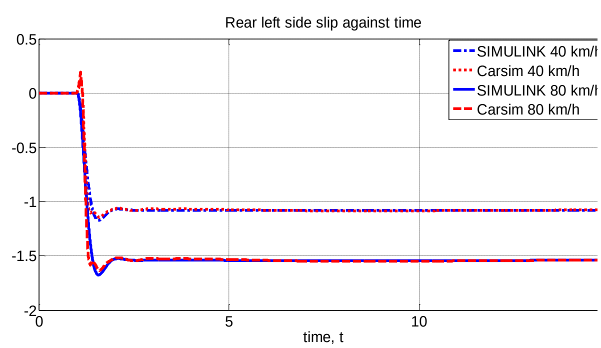

(g) Rear left slip angle against time

Figure 15 Response of the armored vehicle for step steer test at 60 km/h and 80 km/h

3.3 Verification Results in Longitudinal Direction

The verification procedure for longitudinal direction is evaluated using sudden throttle and sudden brake testing. Three types of throttle input condition are used in these verification procedures which are full throttle (100% input), half throttle (50% input) and lastly quarter throttle (25% input) and applied full brake (100% input) for each condition. In this procedure, the armored vehicle is assumed to accelerate in the longitudinal direction without any steering input given. Hence, the response acting in lateral direction can be neglected. In sudden acceleration and braking test, the armored vehicle starts to accelerate from zero velocity until the 40th second and sudden brake is applied to generate brake torque to each wheel. The brake torques is created at all wheels and halts the motion of these wheels simultaneously.

As previous condition, each of the results are compared and evaluated using the root mean square (RMS) analysis for both simulation and validated CarSim model to measure the percentage of errors. Figures 16(a) to 16(f) show the response of the armored vehicle during the sudden acceleration at full throttle and sudden braking at the 40th second. The vehicle starts to accelerate and reach a velocity of 145 km/h at the 40th second and full brake is applied until the vehicle halts. Meanwhile, all the four wheels start to lock once the brake torque is applied and slide without rolling until the vehicle stops. These causes the four wheels to undergo slip condition on a normal road surface.

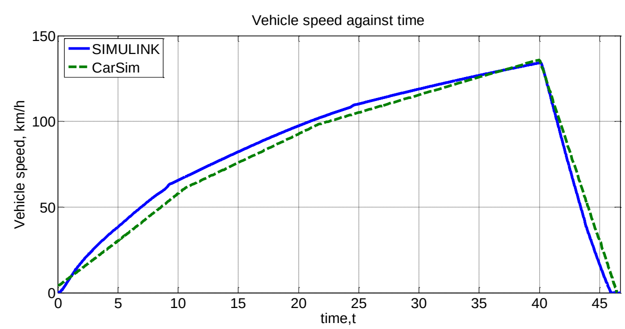

(a) Vehicle velocity against time

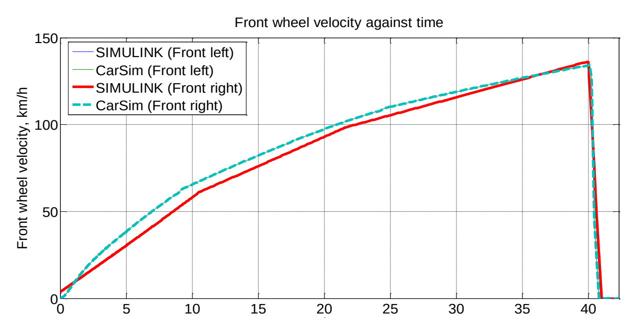

(b) Front wheel velocity against time

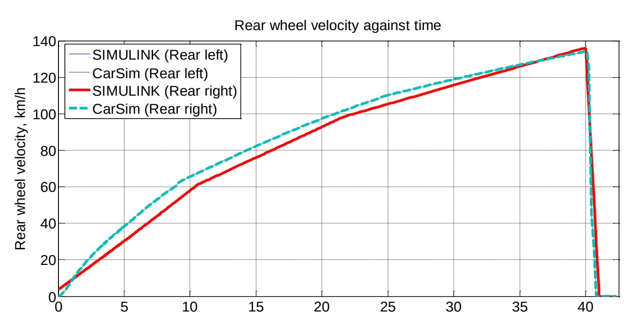

(c) Rear wheel velocity against time

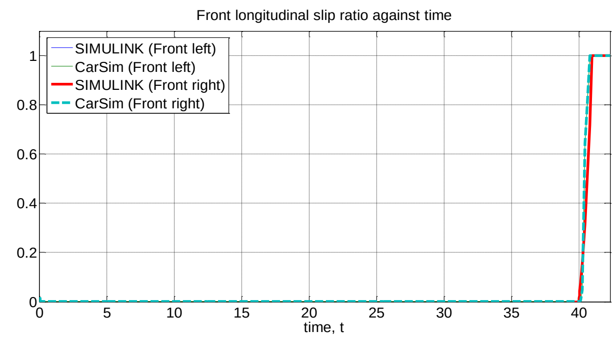

(d) Front longitudinal slip against time

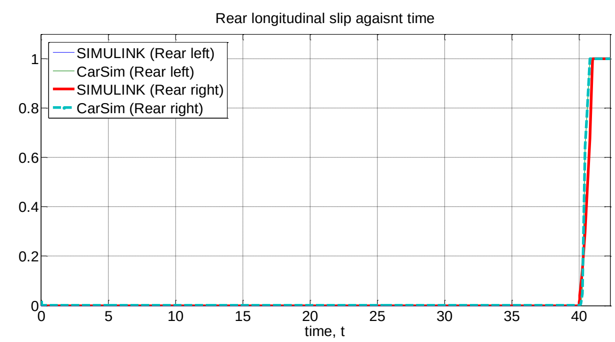

(e) Rear longitudinal slip against time

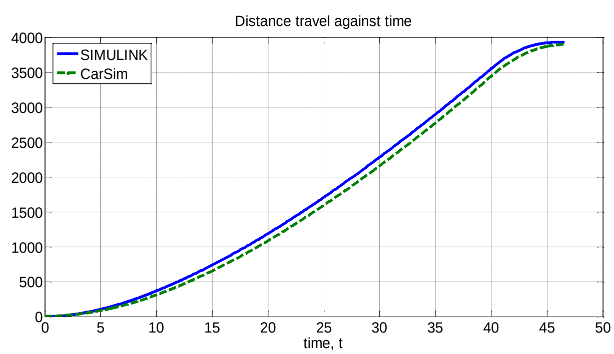

(f) Distance travel against time

Figure 16 Response of the armored vehicle for sudden acceleration (100%) and braking test

The slip in each wheel also increases the stopping distance of the vehicle. In terms of vehicle and wheel velocity, a satisfied comparison is observed between simulation and the CarSim model once the vehicle starts to accelerate until the vehicle decelerates at 46.5 second as shown in Figures 16(a), 16(b) and 16(c). The percentage RMS errors for the vehicle and wheel velocities at the front and rear are 10.54%, 8.73% and 9.36% respectively. Besides, the percentage error for the front and rear longitudinal slip responses as shown in Figure 16(d) and Figure 16(e) which are 7.80% and 7.77%.. The trend of the simulation model closely follows the CarSim response with some minor differences. Besides, the distance travelled as shown in Figure 16(f), for both simulation and CarSim response shows similar response with percentage RMS error of 8.34%. The differences occurred in the simulation model since the pitch moment effect due to braking has been neglected in the simulation model. Even though the pitch moment effect is not considered in this simulation model, the responses are still within the reasonable region as shown in Table 5.

The results of sudden acceleration at 50% throttle input and sudden braking test as shown in Figure 17 indicate that the simulation and CarSim model show similar performance with a small RMS error. The performance comparison are tabulated in Table 5. In terms of vehicle and wheel velocities, the maximum percentage of errors using RMS analysis is 11.79%. Meanwhile, the percentage of RMS error for the front and rear longitudinal slips and distance travel is 4.01%, 6.35% and 8.31% respectively. According to the analysis of the verification results, it is clearly shown that the simulation model is able to follow closely the CarSim model with small deviance. The pitch moment effect is neglected in the simulation model since the vehicle ride model is not considered during sudden acceleration and braking condition.

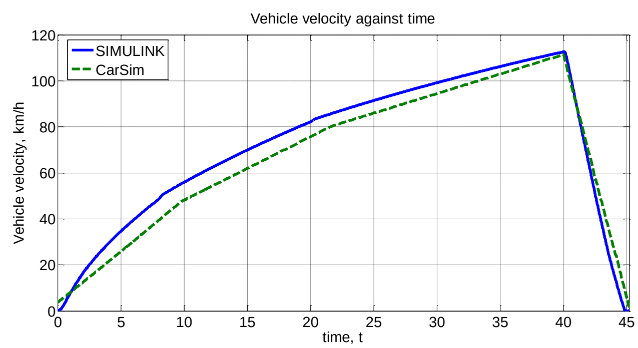

(a) Vehicle velocity against time

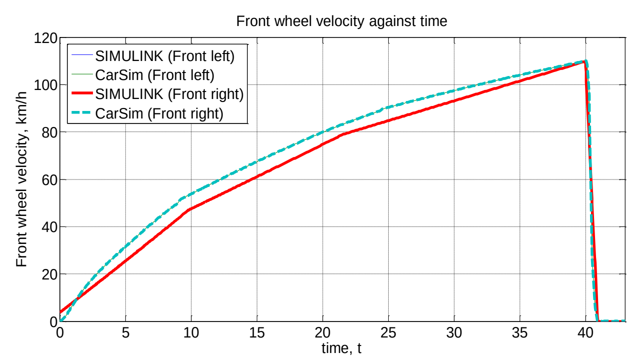

(b) Front wheel velocity against time

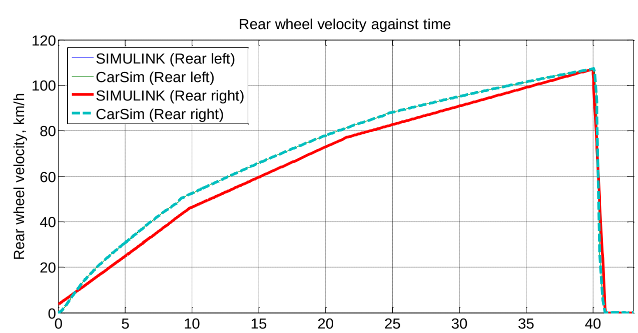

(c) Rear wheel velocity against time

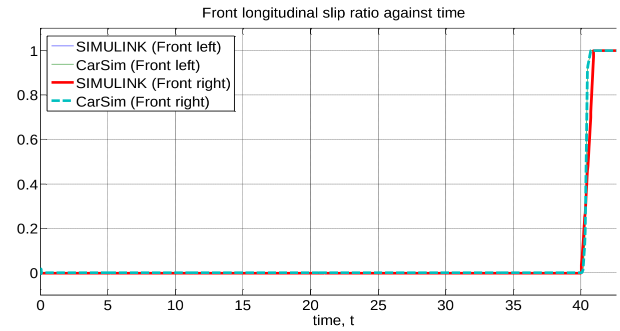

(d) Front longitudinal slip against time

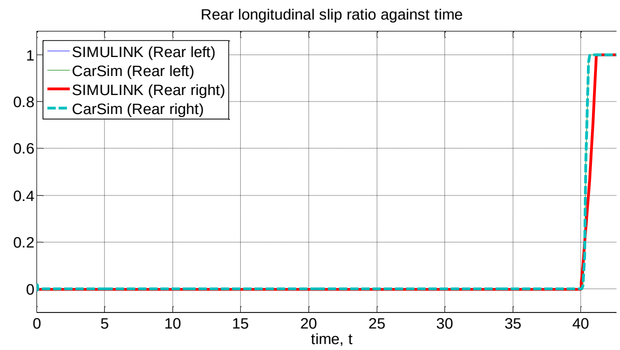

(e) Rear longitudinal slip against time

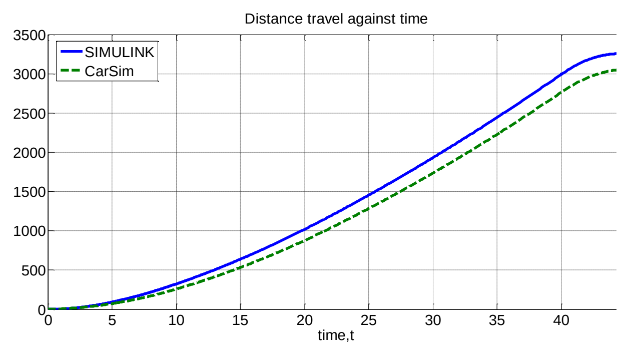

(f) Distance travel against time

Figure 17 Response of the armored vehicle for sudden acceleration (50%) and braking test

Likewise, the results of sudden acceleration at quarter throttle and sudden braking also exhibit similar behavior between simulation model and CarSim model as shown in Figure 18. The maximum percentage of RMS error in term of the velocity of the vehicle and also wheels are 8.69%. Meanwhile, the distance travel of the vehicle and longitudinal slips in front and rear wheels is 8.09%, 2.88% and 7.06% respectively. Overall, it can be concluded that the trends between simulation model and CarSim model are almost similar with acceptable range of RMS error. However, the error could be minimized by adjusting the parameters of the vehicle and tire properties. But this adjustment can be neglected since in control oriented model, the trend of of the response of the vehicle model needs to be satisfied. Henceforth, this 9-DOF armored vehicle model can be used for further controller implementation stage either in lateral or longitudinal direction.

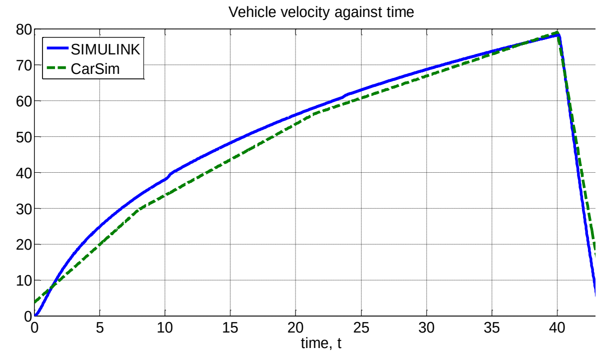

(a) Vehicle velocity against time

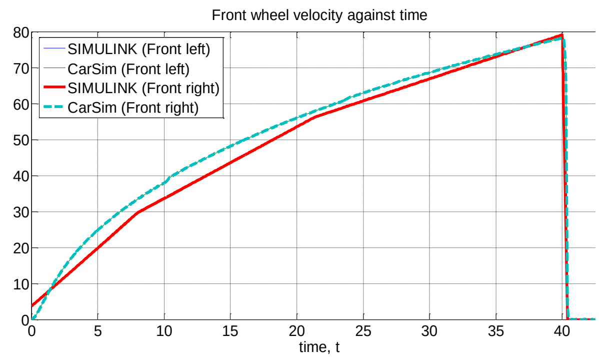

(b) Front wheel velocity against time

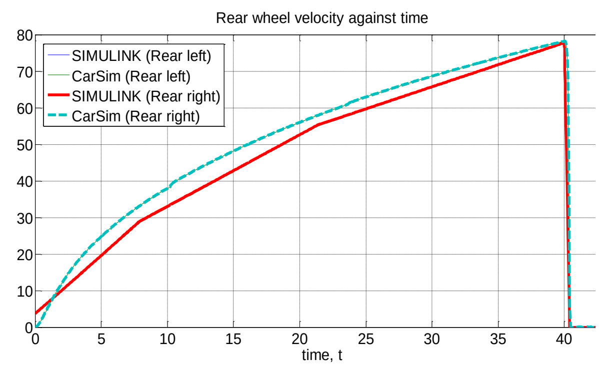

(c) Rear wheel velocity against time

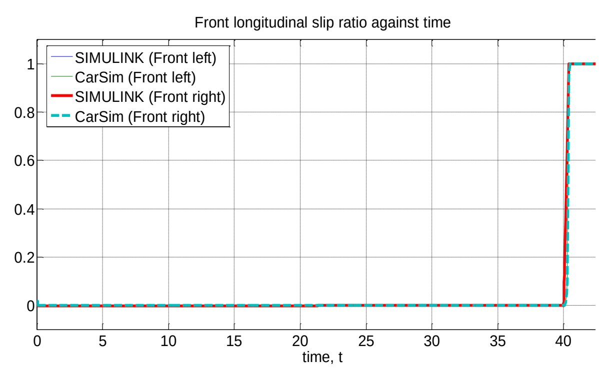

(d) Front longitudinal slip against time

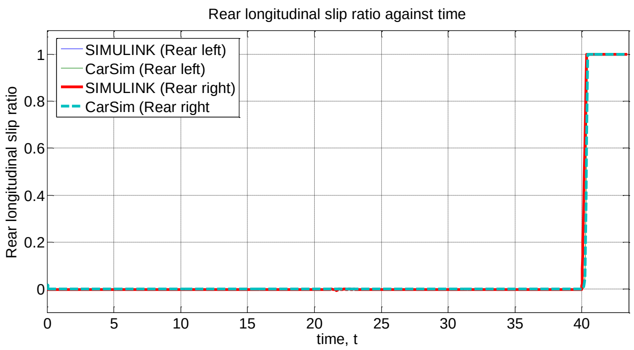

(e) Rear longitudinal slip against time

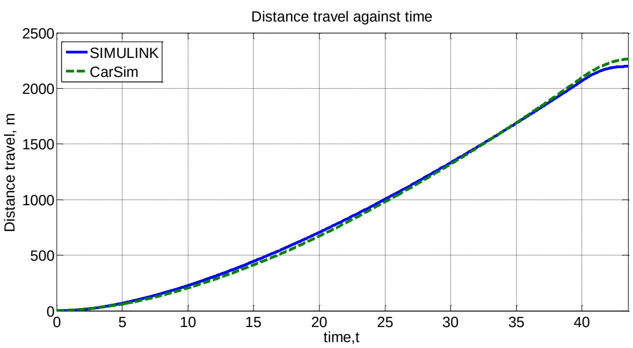

(f) Distance travel against time

Figure 18 Response of the armored vehicle for sudden acceleration (25%) and braking test

4.0 CONCLUSION

In this article, a 9-DOF armored vehicle model which consists of vehicle load distribution, Pacejka Magic tire, handling, lateral and longitudinal slip subsystems has been developed. Three sub-systems which are Pitman arm steering, internal combustion engine and hydraulic brake providing inputs to the vehicle model are mainly considered in the simulation work to analyze the performance of the vehicle model in lateral and longitudinal directions. A validated simulator, CarSim software is used in this study to compare the performance of the developed 9-DOF armored vehicle model in lateral and longitudinal motion. An armored vehicle model, HMMWV, is used as a reference to verify the simulation model. In lateral direction, three types of procedures which are double lane change, slalom and 60 degree step steer at 40 km/h and 80 km/h have been used. Meanwhile, sudden acceleration and braking procedure have been used for longitudinal direction testing where three types of sudden acceleration are considered which are full, half and quarter throttle inputs. The behavior of the vehicle considered during lateral direction is yaw rate, lateral acceleration, vehicle side slip and tire side slip angle. Meanwhile, vehicle and wheel longitudinal tire slip and also the distance travelled by the vehicle are considered in the longitudinal direction. The results of the verification show satisfactory performance of the developed model compared with a validated CarSim model with acceptable error.

Acknowledgement

This work is part of a research project entitled "Robust Stabilization of Armored Vehicle Firing Dynamic Using Active Front Wheel Steering System". This research is fully supported by LRGS grant (No. LRGS/B-U/2013/UPNM/DEFENSE & SECURITY – P1) lead by Associate Professor Dr. Khisbullah Hudha. The authors would like to thank the Malaysian Ministry of Science, Technology and Innovation (MOSTI), MyPhD programme from Minister of Education and National Defense Universiti of Malaysia for their continuous support in the research work. This financial support is gratefully acknowledged.

References

[1] Aparow, V. R., Hudha, K., Ahmad, F. and Jamaluddin, H. 2014. Development of Antilock Braking System using Electronic Wedge Brake Model. *Journal of Mechanical Engineering and Technology*. 6(1): 37-63.

[2] Kushairi, S., Schmidt, R., Omar, A. R., Isa, A. A. M. and Hudha, K. 2014. Tractor–trailer Modelling And Validation. *International Journal of Armored Vehicle Systems*. 21(1): 64-82.

[3] Kruczek, A. and Stribrsky, A. 2004. A Full-Car Model For Active Suspension-Some Practical Aspects. *Proceedings of the IEEE International Conference In Mechatronics*. 41-45.

[4] Yoshimura, T., Kume, A., Kurimoto M. and Hino, J. 2001. Construction Of An Active Suspension System Of A Quarter Car Model Using The Concept Of Sliding Mode Control. *Journal of Sound and Vibration*. 239(2): 187-199.

[5] Litak, G., Borowiec, M., Friswell, M. I. and Szabelski, K. 2008. Chaotic Vibration Of A Quarter-Car Model Excited By The Road Surface Profile. *Communications in Nonlinear Science and Numerical Simulation*. 13(7): 1373-1383.

[6] Türkay, S. and Akçay, H. 2005. A Study Of Random Vibration Characteristics Of The Quarter-Car Model. *Journal of Sound And Vibration*. 282 (1): 111-124.

[7] Tusset, A. M., Rafikov, M. and Balthazar, J. 2009. An Intelligent Controller Design For Magnetorheological Damper Based On A Quarter–Car Model. *Journal of Vibration and Control*. 15(12): 1907-1920.

[8] Jansen, S. T., Zegelaar, P. W. and Pacejka, H. B. 1999. The Influence Of In-Plane Tyre Dynamics On ABS Braking Of A Quarter Vehicle Model. *Vehicle System Dynamics*. 32(2-3): 249-261.

[9] Aparow, V. R., Ahmad, F. Hassan, M. Z. and Hudha, K. 2012. Development of Antilock Braking System Based on Various Intelligent Control System. *Applied Mechanics and Materials*. 229: 2394-2398.

[10] Tur, O., Ustun, O. and Tuncay, R. N. 2007. An Introduction To Regenerative Braking Of Electric Vehicles As Anti-Lock Braking System. *Intelligent Vehicles Symposium, IEEE*. 944-948.

[11] Rauh, J. 2003. Virtual Development Of Ride And Handling Characteristics For Advanced Passenger Cars. *Vehicle System Dynamics*. 40(1-3): 135-155.

[12] Zin, A., Sename, O. Basset, M, Dugard, L. and Gissinger, G. 2004. A Nonlinear Vehicle Bicycle Model For Suspension And Handling Control Studies. *Proceedings Of The IFAC Conference On Advances In Vehicle Control And Safety*. AVCS. 638-643.

[13] Meijaard, J. P. and Schwab, A. L. 2006. Linearized Equations For An Extended Bicycle Model. *III European*

Conference on Computational Mechanics. Springer Netherlands. 772-790.
[14] Baslamisli, S. C., Polat, I. and Kose, I. E. 2007. Gain Scheduled Active Steering Control Based On A Parametric Bicycle Model. *Intelligent Vehicles Symposium*, IEEE. 1168-1173.
[15] Thompson, A. G. and Pearce, C. E. M. 2001. Direct Computation Of The Performance Index For An Optimally Controlled Active Suspension With Preview Applied To A Half-Car Model. *Vehicle System Dynamics*. 35(2): 121-137.
[16] Gao, W., Zhang, N. and Du, H. P. 2007. A Half Car Model For Dynamic Analysis Of Vehicles With Random Parameters. *Australasian Congress on Applied Mechanics*. ACAM, Brisbane, Australia.
[17] Huang, J. L. and Chen, C. 2010. Road-Adaptive Algorithm Design Of Half-Car Active Suspension System. *Expert Systems with Applications*. 37: 305-312.
[18] Ahmad, F., Hudha, K., Imaduddin, F. and Jamaluddin, H. 2010. Modelling, Validation And Adaptive PID Control With Pitch Moment Rejection Of Active Suspension System For Reducing Unwanted Vehicle Motion In Longitudinal Direction. *International Journal of Vehicle Systems Modelling and Testing*. 5(4): 312-346.
[19] Hudha, K. Kadir, Z. A. and Jamaluddin, H. 2014. Simulation And Experimental Evaluations On The Performance Of Pneumatically Actuated Active Roll Control Suspension System For Improving Vehicle Lateral Dynamics Performance. *International Journal of Vehicle Design*. 64(1): 72-100.
[20] Aparow, V. R., Ahmad, F., Hudha, K. and Jamaluddin, H. 2013. Modelling And PID Control Of Antilock Braking System With Wheel Slip Reduction To Improve Braking Performance. *International Journal of Vehicle Safety*. 6(3): 265-296.
[21] Hudha, K., Jamaluddin, H. and Samin, P. M. 2008. Disturbance Rejection Control Of A Light Armoured Vehicle Using Stability Augmentation Based Active Suspension System. *International Journal of Armored Vehicle Systems*. 15(2): 152-169.
[22] Trikande, M. W., Jagirdar, V. V. and Sujithkumar, M. 2014. Modelling and Comparison of Semi-Active Control Logics for Suspension System of 8x8 Armoured Multi-Role Military Vehicle. *Applied Mechanics and Materials*. 592: 2165-2178.
[23] Hudha, K., Kadir, Z. A. Said, M. R. and Jamaluddin, H. 2009. Modelling, Validation And Roll Moment Rejection Control Of Pneumatically Actuated Active Roll Control For Improving Vehicle Lateral Dynamics Performance. *International Journal of Engineering Systems Modelling and Simulation*. 1(2): 122-136.
[24] Ikenaga, S., Lewis, F. L., Campos, J. and Davis, L. 2000. Active Suspension Control Of Ground Vehicle Based On A Full Vehicle Model. *Proceedings of the 2000 American Control Conference*. Illinois, Chicago. 28–30 June. 6: 4019-4024.
[25] Short, M., Pont, M. J. and Huang, Q. 2004. Safety and Reliability of Distributed Embedded Systems Simulation of Vehicle Longitudinal Dynamics, ESL Technical Report, University of Leicester.
[26] Bakker, E. Pacejka, H. and Lidnar, L. 1987. A New Tire Model With Application In Vehicle Dynamic Studies. *SAE Technical Paper*, 890087. 101-113.
[27] Ping, E. P., Hudha, K. and Jamaluddin, H. 2010. Automatic Steering Control For Lanekeeping Manoeuvre: Outer-Loop And Inner-Loop Control Design. *International Journal of Advanced Mechatronic Systems*. 2(5): 350-368.
[28] Pacejka, H., Bakker, E. and Nyborg, L. 1987. Tyre Modelling For Use In Vehicle Dynamics Studies. *SAE Technical Paper*, 870421.
[29] Shwetha, G. N., Ramesh, H. R. and Shankapal, S. R. 2013. Modeling, Simulation And Implementation Of A Proportional-Derivative Controlled Column-Type EPS. *International Journal of Enhanced Research in Science Technology & Engineering*. ISSN: 2319-7463. 2(9): 10-19.
[30] Liu, A. and Chang, S. 1995. Force Feedback In A Stationary Driving Simulator. *Systems, Man and Cybernetics, IEEE International Conference on Intelligent Systems for the 21st Century*. 2: 1711-1716.
[31] Proca, A. K. 1998. Identification Of Power Steering System Dynamic Models. *Mechatronics*. 8(3): 255-270.
[32] Karnopp, D. Argolis, R. and Rosenberg, R. 2000. *System Dynamis: Modeling and Simulations of Mechatronic Systems*. New York, NY: John Wiley Sons.
[33] Moskwa, J. J.and Hedrick, J. K. 1992. Modeling And Validation Of Automotive Engines For Control Algorithm Development. *ASME Journal of Mechanisms, Transmissions and Automation in Design*. 114(2): 278-285.
[34] Wahlström, J., and Eriksson, L. 2011. Modelling Diesel Engines With A Variable-Geometry Turbocharger And Exhaust Gas Recirculation By Optimization Of Model Parameters For Capturing Non-Linear System Dynamics. *Proceedings of the Institution of Mechanical Engineers, Part D: Journal of Automobile Engineering*. 225(7): 960-986.
[35] Hedrick, J. K., Mcmahnon, D., Swaroop, D., Garg, V., Maciuca, D., Blackman, T. and Yip, P. 1995. Longitudinal Control Development for IVHS Fully Automated and Semi automated Systems- Phase 1, PATH Research Report, University of California, Berkeley.
[36] True, H. (Ed.). 2003. *The Dynamics of Vehicles on Roads and on Tracks*. CRC Press Publisher. 37.
[37] Udas, A. 2011. *Road Variability And Its Effect On Vehicle Dynamics Simulation*. MSc thesis, University of Iowa, Iowa.
[38] Toffin, D. Reymond, G. Kemeny, A. and Droulez, J. 2003. Influence Of Steering Wheel Torque Feedback In A Dynamic Driving Simulator. *Proceedings of the driving simulation conference*. October, North America, Dearborn, USA.

Appendix

Table 1 Parameter of vehicle model

Description	Symbol	Value
Wheel inertia	I_ω	15 $\mathrm{kg.m^2}$
Frontal area	A	0.05$\mathrm{m^2}$
Vehicle mass	m	2210 kg
Wheel mass	m_w	100 kg
Tire radius	R_w	0.468 mm
Gravitational acceleration	g	9.81 m/s^2
Aerodynamic resistance	C_d	0.29
Rolling resistance	C_r	0.01
Front length from COG	l_f	1070 mm
Rear length from COG	l_r	2230 mm
Height of vehicle from COG	h	660 mm
Vehicle width	t	1900 mm
Yaw inertia	I_{yaw}	4300 $\mathrm{kg.m^2}$

Table 2 Parameter of the Pitman arm steering model

Description	Symbol	Value
Moment of inertia of steering wheel	J_{sw}	0.035 kg $\mathrm{m^2}$
Viscous damping of steering wheel	B_{sw}	0.36 Nm/ (rad/sec)
Steering column rotational stiffness	K_{sc}	42000 Nm/rad
Angular displacement due to universal joint	θ_k	20°
Steering arm length	l_s	0.2 m
Return pressure	P_o	0 N/$\mathrm{m^2}$
Pump flow rate	Q_s	0.0002 $\mathrm{m^3}$/s
Piston area	A_p	0.005 $\mathrm{m^2}$
Cylinder length	L	0.15 m
Orifice flow coefficient	C_{do}	0.6
Fluid density	ρ	825 kg/m^3
Fluid volume	V_s	8.2$\times 10^{-5}$ $\mathrm{m^3}$
Fluid bulk modulus	β_f	7.5 $\times 10^8$ $\mathrm{N/m^2}$
Torsion bar rotational stiffness	K_{tr}	35000 Nm/rad
Sector gear ratio	τ_{sg}	0.5
Moment of inertia of steering column	J_{sc}	0.055 kg $\mathrm{m^2}$
Viscous damping of steering column	B_{sc}	0.26 Nm/ (rad/sec)
Coulomb friction breakout force on steering linkage	C_{SL}	0.5 N
Gear ratio efficiency of forward transmission	η_f	0.985
Gear ratio efficiency of backward transmission	η_B	0.985
Steering rotational stiffness due to linkage and bushing	K_{SL}	15500 Nm/rad
Metering orifice	A_1 and A_2	2.5 $\mathrm{mm^2}$

Table 3 Parameter of the engine dynamics model

Description	Symbol	Value
the maximum flow rate corresponding to full open throttle	MAX	0.1843 kg/s
intake manifold volume	V_m	0.0038 m^3
Intake engine volume	V_e	0.0027 m^3
effective inertia of the engine	I_e	0.1454 kg m^3
maximum torque production capacity of an engine	c_T	498636 Nm/(kg/s)
Temperature of manifold	T_m	300 deg K
Mass of the air intake	M_a	28.84 g/mole
Gas constant	R	8314.3 J/mole deg k
intake to torque production delay	Δt_{it}	5.48/ ω_e
spark to torque production delay	Δt_{st}	1.30/ ω_e

Table 4 Percentage of error using RMS value for lateral motion

ARMORED VEHICLE IN LATERAL DYNAMICS							
Case Procedure	**Observation data**	**ROOT MEAN SQUARE (RMS)**				**Percentage Error (%)**	
		SIMULATION		**CARSIM**			
		40 km/h	80 km/h	40 km/h	80 km/h	40 km/h	80 km/h
Double lane change	lateral acceleration	0.0576	0.09186	0.0551	0.09605	4.55	4.56
	yaw rate	0.4352	0.7687	0.4612	0.7253	5.64	5.65
	vehicle body side slip	0.1701	0.2483	0.1551	0.2981	9.67	11.10
	front left side slip	0.2328	0.4238	0.2543	0.3881	9.22	8.42
	front right side slip	0.2336	0.4238	0.2543	0.3893	8.13	8.15
	rear left side slip	0.1728	0.2552	0.1531	0.2881	11.41	11.41
	rear right side slip	0.1728	0.2552	0.1531	0.2881	11.41	11.41
Slalom	lateral acceleration	0.02485	0.04042	0.02471	0.04063	0.56	0.52
	yaw rate	0.04166	0.0694	0.04134	0.0689	0.77	0.76
	vehicle body side slip	0.01778	0.02595	0.01907	0.02236	6.76	8.17
	front left side slip	0.00866	0.01444	0.00819	0.0137	5.74	5.13
	front right side slip	0.00857	0.01464	0.00811	0.0127	5.67	6.70
	rear left side slip	0.00695	0.01207	0.0066	0.011	5.05	8.87
	rear right side slip	0.00687	0.01227	0.00651	0.012	5.38	8.04
Step Steer at 60 Deg	lateral acceleration	0.211055	0.3247	0.211835	0.3259	0.36	0.37
	yaw rate	9.0285	13.89	8.5995	13.23	5.23	4.75
	vehicle body side slip	0.99905	1.537	1.0257	1.578	2.59	2.66
	front left side slip	1.04975	1.615	1.144	1.76	8.24	8.98
	front right side slip	0.99125	1.525	1.08875	1.675	8.96	9.10
	rear left side slip	1.01725	1.565	1.04325	1.605	2.45	2.45
	rear right side slip	1.014	1.56	1.03675	1.595	2.19	2.19

Table 5 Percentage of error using RMS value for lateral motion

LONGITUDINAL MOTION				
Case Procedure	**Observation dynamic behavior**	**Root Mean Square (RMS)**		**Percentage Error (%)**
		Simulation	**CarSim**	
Full throttle then brake	vehicle velocity	0.04348	0.0486	10.54
	front wheel velocity	0.04312	0.04765	10.51
	rear wheel velocity	0.04265	0.0476	11.61
	distance travel	3924	4281	8.34
	front longitudinal slip	0.08382	0.07775	7.80
	rear longitudinal slip	0.07775	0.07171	7.77
Half throttle then brake	vehicle velocity	0.04258	0.0476	11.79
	front wheel velocity	0.04378	0.0476	8.73
	rear wheel velocity	0.04265	0.0466	9.36
	distance travel	3224	2956	8.31
	front longitudinal slip	0.07575	0.07271	4.01
	rear longitudinal slip	0.07982	0.07475	6.35
Quarter throttle then brake	vehicle velocity	0.04118	0.04476	8.69
	front wheel velocity	0.04221	0.04503	6.68
	rear wheel velocity	0.04023	0.04231	5.17
	distance travel	2250	2432	8.09
	front longitudinal slip	0.07425	0.07211	2.88
	rear longitudinal slip	0.07765	0.07217	7.06